Proc. Lunar Sci. Conf. 7th (1976), p. 1087–1112.
Printed in the United States of America

Photometric studies of light scattering above the lunar terminator from Apollo solar corona photography

J. E. McCoy

NASA Johnson Space Center, Houston, Texas 77058

Abstract—Excess brightness is found in 70 mm photographs of the solar corona above the lunar terminator during Apollo 15 and Apollo 17. Maximum brightness of this scattered light is determined from calibration of image density to be in excess of 10^{-3} cd/cm^2. The observed excess brightness displays circular symmetry above the lunar horizon subsolar point, characteristic of forward diffraction scattering from micron or submicron size (solid) grains, and decays rapidly in intensity with altitude and distance from the lunar terminator. The observed brightness cannot be accounted for by a co-orbiting cloud of spacecraft contaminants, but requires a variable lunar dust "atmosphere" over the terminator regions with an integrated vertical column density exceeding 10^{-9} g/cm^2 extending to altitudes in excess of 100 km. To maintain such large masses of lunar fines above the terminator requires either local mass churning rates in excess of 2×10^{-11} g/cm^2 sec or the assumption of some degree of high altitude electrostatic suspension to increase the dwell time of individual grains at the altitudes observed. Such a model would reduce mass churning rates while causing selective erosion/deposition and potential for escape of significant mass from the moon.

Introduction

The moon was expected to be an ideal location to observe the solar corona/zodiacal light (CZL) over its full extent. Light scattered in the earth's atmosphere confines studies of the inner corona to within a few solar radii of the limb, even during solar eclipse observations. All observations require correction for the stray light scattered in, for atmospheric absorption and even for nighttime airglow in the zodiacal light measurements. These corrections introduce significant uncertainties even where measurements were obtainable. Observations from the moon, either surface or orbit, would eliminate the problem of an intervening atmosphere. By observing across the terminator, with the instrument in darkness, the problems of light scattering within the instrument are also reduced by a factor of about 10^6.

It was generally accepted that no detectable lunar "twilight" or night sky illumination would be present. Therefore, with the sun and any brighter inner portions of the CZL occulted by the moon, each point in the CZL could be studied as it appeared just above the lunar horizon. No provision for large dynamic range would be needed, the exposure or other instrument parameters could be adjusted just to match the brightness of the point being studied. A series of photographic experiments were conducted from lunar orbit for this purpose during the Apollo program (Dunkelman *et al.*, 1972; MacQueen *et al.*, 1972; MacQueen *et al.*, 1973). Observations were also attempted from the lunar surface using the Surveyor TV camera after sunset (Bohlin, 1971), and by the Soviet Lunokhod (astronomical

sky-brightness) photometer (Severny *et al.*, 1973). The lunar orbital photography during the Apollo 16 mission was highly successful (MacQueen *et al.*, 1973a), extending our knowledge of the solar corona intensity to elongations in excess of 40 $R_\odot$ and greatly reducing the uncertainty in absolute value of the inner brightness values previously observed. This was done by comparing corona image densities in a series of 70 mm photographs made, at progressively decreasing exposure values, as the brighter portions of the corona rose above the horizon approaching orbital sunrise. The ability to cross-check between successive frames allowed verification of camera/lens/film calibrations as well as the absence of any (variable) stray light contamination from frame to frame.

Analysis of the Apollo solar corona photography does not always work out with that expected simplicity. It would appear there is frequently present an additional, time varying, contribution to the light observed many kilometers above the lunar terminator. This first seemed likely based on various visual reports by the Apollo crews, particularly sketches by the Apollo 17 crew (McCoy and Criswell, 1974). Preliminary analysis of the Apollo 15 solar corona photographs had shown the existence of coronal "streamer" structures which could be correlated with K-coronameter intensity features in the innermost corona (Wilson and MacQueen, 1974), but reliable brightness estimates had not been obtained due to failure of values obtained at a given point to reproduce from frame to frame (Ross, pers. comm.). This failure was assumed due to the presence of "stray" light contamination and/or use of incorrect exposure settings. Reinterpretation, based on preliminary densitometer analysis of four Apollo 15 solar corona photographs, resulted in the first quantitative evidence (McCoy *et al.*, 1975) showing the presence of a locally scattered component of light, from a source extending several kilometers above the lunar terminator. The time and spatial behavior of excess brightness over the nominal CZL was similar to that inferred by McCoy and Criswell (1974) from the Apollo 17 crew visual observations.

To verify the initial photometric result and extend the study to other times, the entire set of 70 mm solar corona photography and associated calibration exposures were redigitized using the microdensitometer facilities at NASA/JSC. Film calibrations were cross-checked between the HAO and JSC standards and also between missions. The results have been applied to the Apollo 15 and Apollo 17 photo sequences, and show clearly the presence of an additional component of light from above the lunar terminator superimposed on the solar CZL at the time of the Apollo 15 and 17 photos. This component is evident on the basis of absolute intensity near the terminator, progressive decrease with (time or) distance from the terminator, and a distinct departure of symmetry near the horizon from eliptical about the ecliptic (characteristic of the CZL) toward circular above the point on the horizon directly above the sun (characteristic of scattering by a local cloud of particles above the terminator).

Film Scanning and Calibration

Three 70 mm photo sequences were available from Apollo 15, one "sunset" sequence (frames 318–325) from which the original set of four frames were analyzed in (McCoy *et al.*, 1975) plus two "sunrise" sequences viewing the corona over the opposite terminator (frames 310-316 and 377-384). Absolute calibration references for these frames were obtained from a series of seven post-flight exposures of the HAO (High Altitude Observatory, NCAR, Boulder) standard illuminated step-wedge (Pizzo and Gosling, 1972), cross-checked against pre- and post-flight exposures of the standard JSC 21-step density wedge. Two "sunrise" sequences were available from Apollo 16 (frames 885-891 and 904-910, taken April 22–23, 1972), plus one "sunrise" sequence from Apollo 17 (frames 647-653, taken December 12, 1972). The Apollo 16 and 17 flight films contained additional HAO step-wedge exposures to extend the calibration (for reciprocity effects) to longer exposures and lower absolute brightness, as well as the usual JSC standard. All frames were scanned at JSC, with repeat scans for densitometer drift against a single Apollo 15 calibration frame between photo-frames. This provided both an independent verification of the earlier HAO facility results plus direct intercomparability of calibrations from the different missions.

All images were scanned from the original flight films, using the (NASA/JSC I.D. # 96054) "Specscan" System S-3000 microdensitometer. This system measures specular density over a range of 0.00–4.00 D, with a specified stability of ± 0.02D/8 hr and linearity of ± 0.02 D. Positions in X and Y are repeatable ± 1 μm, orthogonal within ± 4 arc sec.

High resolution scans of each solar corona image were made in March, 1975, using a 50 μm spot at $X - Y$ intervals of 50 μm. Reference scans of the Apollo 15 (Mag R) $\frac{1}{8}$ sec post-flight exposure of the HAO calibration standard were made before and after each corona image as a calibration drift check. High resolution scans of each of the post-flight HAO 15-step calibration exposures were made to provide direct calibration reference for the corona images. Graininess of the 2485 film is quite apparent on this (50 μm) scale, resulting in ± 0.1 D random variations from point to point in a uniformly exposed area.

A second series of lower resolution scans were made during June–September 1975 to provide a quick reference data set with lower grain noise and faster processing for general area information. This set includes everything in the high resolution series, rescanned using a 200 μm spot at 200 μm intervals, plus all available calibration wedge images scanned at 50 μm intervals with a 30×400 μm slit. This included all post-flight HAO 15-step wedge images previously scanned with the 50 μm spot. In addition, HAO pre-flight calibration images on Apollo 17 film magazines QQ and RR (which used an incorrect aperture stop) and the standard JSC 21-step wedge pre-flight and post-flight images were included to verify the original Apollo 16 and 17 post-flight calibrations for $\frac{1}{2}$, 1, 4, and 10 sec exposures, which showed extreme and non-linear reciprocity failure. The redundant values indicate that consistent results may be obtained in this region ($B > 2 \times 10^{-10}$ $B_\odot$, density >2.0 D), but only by direct comparison with the density

obtained in a calibration image exposed on the same film at the same intensity and the same shutter speed.

Exposure values required to obtain a film density of 1.0 D were compared between the HAO $\frac{1}{8}$ sec image and the JSC wedge for Apollo 15 (mag R) and Apollo 17 (mag QQ and mag RR). The results agree within 10%, well within the range of probable reciprocity effects. Relative values of density (light intensity incident on the film) appear to be reproducible within ±0.02 D (±3% of B in the linear portion of the *B* vs. *d* curves) for identical exposure conditions (i.e., pre-flight, flight or post-flight). Absolute values of density (brightness) appear to be reliable within ±10%; if obtained by direct comparison to a reference standard exposed on the same film, handled and processed in the same manner, of similar density and scanned on the same equipment. Of these requirements, use of the same exposure intensity and duration plus film handling and processing seem most crucial. This is evidenced by comparison of the identical pre-flight HAO calibration images on each of the Apollo 17 flight film magazines, QQ and RR. Brightness steps in each image on QQ give density values .03 ± .03 D greater than the corresponding image and step on RR. This is less than the differences observed between pre-flight and post-flight exposures of the JSC wedge on each film, which amounted to as much as 10% (0.20 at 1.80/2.00 on RR). This was fortunate, as the only calibration images with a reliable absolute calibration were the post-flight images on mag RR, while the solar corona images were on mag QQ.

The film density recorded for each intensity step of the HAO calibration wedge image was plotted vs. equivalent brightness of that step to provide a direct calibration curve to convert density to apparent brightness at the film plane. One such curve was available for each shutter speed used on Apollo 17, from $\frac{1}{60}$ sec to 10 sec. On Apollo 15, a curve was available for each planned shutter speed from $\frac{1}{125}$ sec to 1 sec. Since the 10 sec exposures on Apollo 15 were obtained by accident, a calibration curve for them had to be fabricated by applying the Apollo 17 reciprocity relation to the Apollo 15 one second data. As noted above, this is a rather uncertain procedure subject to significant error when applied to 2485 film. Brightness values obtained from the Apollo 15 ten sec exposures should be viewed with suspicion.

Observed Brightness

Density values in the CZL images were used, from points located at constant angular distances from the sun along the ecliptic, to determine the corresponding light intensity incident on the film plane at that point in each image. A correction for lens vignetting is then applied, taken from a JSC Camera Calibration Lab test of the 80 mm *f*/2.8 lens S/N 1413. Values are listed in Table 1. A further correction was then made for transmission losses in the lens and spacecraft window. This is the largest source of uncertainty (±30%) in the absolute calibration, as values anywhere from 72% down to 30% are found quoted in various publications and NASA test documents. For these results, I have used the T-stop test results for the Apollo 15 lens 1404 contained in the NASA Calibration Report (LEC/HASD

No. 649D.21.076) of 51% transmission, which seems typical. Taking a mean value of 72% for the window gives a net transmission of 37%. (There is an additional term due to changing angle of incidence through the window from top to bottom of the film frame which is small and constant between frames. It has been ignored due to uncertainty of its exact value and the actual angle of incidence.)

Table 1. Relative illumination of image plane vs. distance above horizon for constant brightness scene.

Film frames	At horiz.	h + 2.5°	h + 5°	h + 10°	h + 15°	h + 20°
Apollo 15 (310-316) along ecliptic	83%	90%	94%	100%	90%	75%
along max. B (10° off ecliptic)	82%	88%	92%	95%	85%	75%
Apollo 15 (318-325)	52%	58%	63%	73%	77%	75%
Apollo 16	80%	85%	90%	90%	80%	67%
Apollo 17	60%	65%	70%	78%	79%	75%

The results of this procedure for the Apollo 15 orbital sunset are shown in Table 2. Brightness at each step in the above procedure is in units of 10^{-12} $B_\odot$ (2×10^{-7} cd/cm^2). As noted previously, the calibration curve used to obtain image brightness ($B_\odot$) from film density (d) for the 10 sec exposure (frame 325) is not entirely reliable, as it is an extrapolation from the 1 sec curve using the reciprocity function observed between the Apollo 17 one and ten sec calibrations. The location of each point in frames 320–325 is quite accurate (within 0.1–0.2 degree) with respect to sun-center and ecliptic plane, due to the availability of star images (particularly Venus, α Gem and β Gem) to precisely define coordinates. Location of points in frames 318 and 319 is less certain, being based on calculated position of the sun below the horizon and image scale. The values of brightness vs. distance from the sun in successive frames are plotted in Fig. 1. The most recent values for the nominal K + F corona are shown as a dashed line for comparison. The solid lines are drawn through the appropriate data points to show the actual brightness recorded by Apollo 15 at times of 17, 33, 54, 66, and 73 sec after sunset. Note the large excess (>500%) brightness at all elongations at 17 sec after sunset, decreasing steadily with time after sunset.

Table 3 and Fig. 2 show similar results for the Apollo 15 orbital sunrise sequence, with brightness increasing as sunrise is approached. Positions determined in frames 310 and 311 are quite accurate due to the availability of star images (particularly Regulus and Jupiter) to define coordinates. Location of points in the other frames is less certain, again based on calculation of the sun's position below the horizon. Of those frames, only 312 is included here as the others were underexposed and contained a useable image only within one degree of the horizon. Again, values in frame 311 are not fully reliable due to use of the extrapolated calibration for the 10 sec exposure. In addition, the 1 sec shutter opening used for frame 310 is uncertain. Frame 311 was a 10 sec exposure due to

Table 2. Apollo 15—70 mm "solar corona"—sunset sequence.

Frame No.	AS15-98-13325 (10 sec)? SS + 93 sec; horiz @ 4.7°				323 ($\frac{1}{4}$ sec) SR + 66 sec; horiz @ 3.3°				322 ($\frac{1}{8}$ sec) SS + 54 sec; horiz @ 2.7°			
Elongation	d	B_0	B_1	B	d	B_0	B_1	B	d	B_0	B_1	B
1°												
2°												
3°									.92	8.5	16.3	44
4°					.70	3.8	7.3	19.7				
5°	2.20	1.7	3.3	8.9	.56	2.7	4.9	13.2	.53	3.5	6.0	16
6°	2.05	1.3	2.36	6.4	.52	2.2	3.6	9.7				
7°	1.84	1.0	1.7	4.6								
8°	1.64	.78	1.3	3.5								
9°	1.48	.65	1.06	2.9								
10°	1.30	.52	.83	2.2								

Frame No.	320 ($\frac{1}{30}$ sec) SS + 33 sec; horiz @ 1.7°				319 ($\frac{1}{60}$ sec) SS + 28 sec; horiz @ 1.4°				318 ($\frac{1}{125}$ sec) SS + 17 sec; horiz @ 0.9°			
Elongation	d	B_0	B_1	B	d	B_0	B_1	B	d	B_0	B_1	B
1°									1.16	150	290	780
1½°					.87	60	115	310	.76	80	150	410
2°	1.04	40	77	208	.70	45	82	220	.62	53	96	260
3°	.68	20	36	97	.52	22	38	103				
4°	.50	10	17	46								
5°	.47	7	12	32								

Table 3. Apollo 15—70 mm "solar corona"—sunrise sequence.

Frame No.	AS15-98-13310 (1 sec)? SR-60 sec; horiz @ 3.0°				AS15-98-13311 (10 sec)? SR-50 sec; horiz @ 2.5°				AS15-98-13312 ($\frac{1}{8}$ sec) SR-40 sec; horiz @ 2.0°			
Elongation	d	B_0	B_1	B	d	B_0	B_1	B	d	B_0	B_1	B
1°												
2°									(.73)	(6.3)	(10.0)	(27)
3°					2.50	4.0	4.8	13.0	.67	5.6	6.7	18.0
4°	.98	2.0	2.3	6.2	2.45	3.5	4.0	10.8	.60	4.7	5.4	14.6
5°	.32	1.6	1.78	4.8	2.35	2.5	2.8	7.6	.54	3.8	4.3	11.6
6°	.70	1.3	1.43	3.9	2.25	1.8	1.98	5.4	.51	3.1	3.4	9.2
7°	.64	1.10	1.18	3.2	2.10	1.5	1.61	4.4				
8°	.56	.90	.96	2.6	2.00	1.2	1.28	3.5				
9°					1.90	1.08	1.10	3.0				
10°					1.80	.95	.95	2.6				

incorrect operation of the 70 mm camera's shutter/electric film advance feature, resulting in an open shutter on frame 311 for the 10 sec interval between planned exposures in addition to the $\frac{1}{2}$ sec interval intended. It is believed that this affected only frame 311 and not the adjacent frame.

Table 4 and Fig. 3 show similar results for the Apollo 17 orbital sunrise sequence. The excess light present over the nominal (Apollo 16) CZL values is

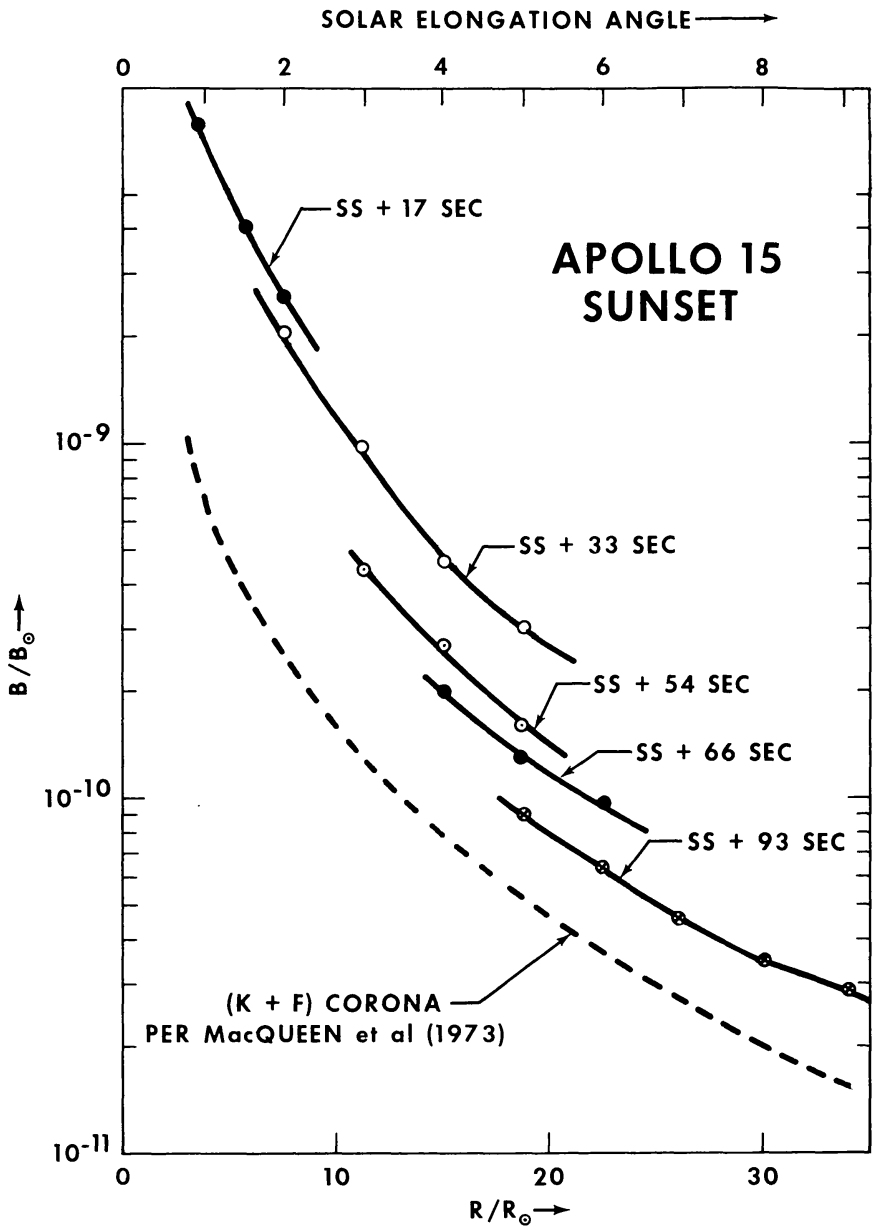

Fig. 1. Observed brightness in "solar corona" images (units of mean brightness of solar disk, $B_\odot$) vs. distance from sun center in sequence of 5 photo frames exposed 17, 33, 54, 66, and 93 sec after orbital sunset. Apollo 15 orbit 24, 18:43 GMT, July 31, 1971.

less than observed on Apollo 15, confined to lower altitudes and showing a rather different (layered?) altitude profile.

Further verification of the presence during Apollo 15 of a dominant fraction of light from scattering above the terminator is observed in Fig. 4, which is a selection of computer generated isointensity profiles above the lunar horizon from each mission. The positions of sun, ecliptic plane, and local vertical are indicated. Note the distinct symmetry about the ecliptic plane in the Apollo 16 and Apollo 17 frames, where the nominal CZL dominates the recorded brightness. Compare this

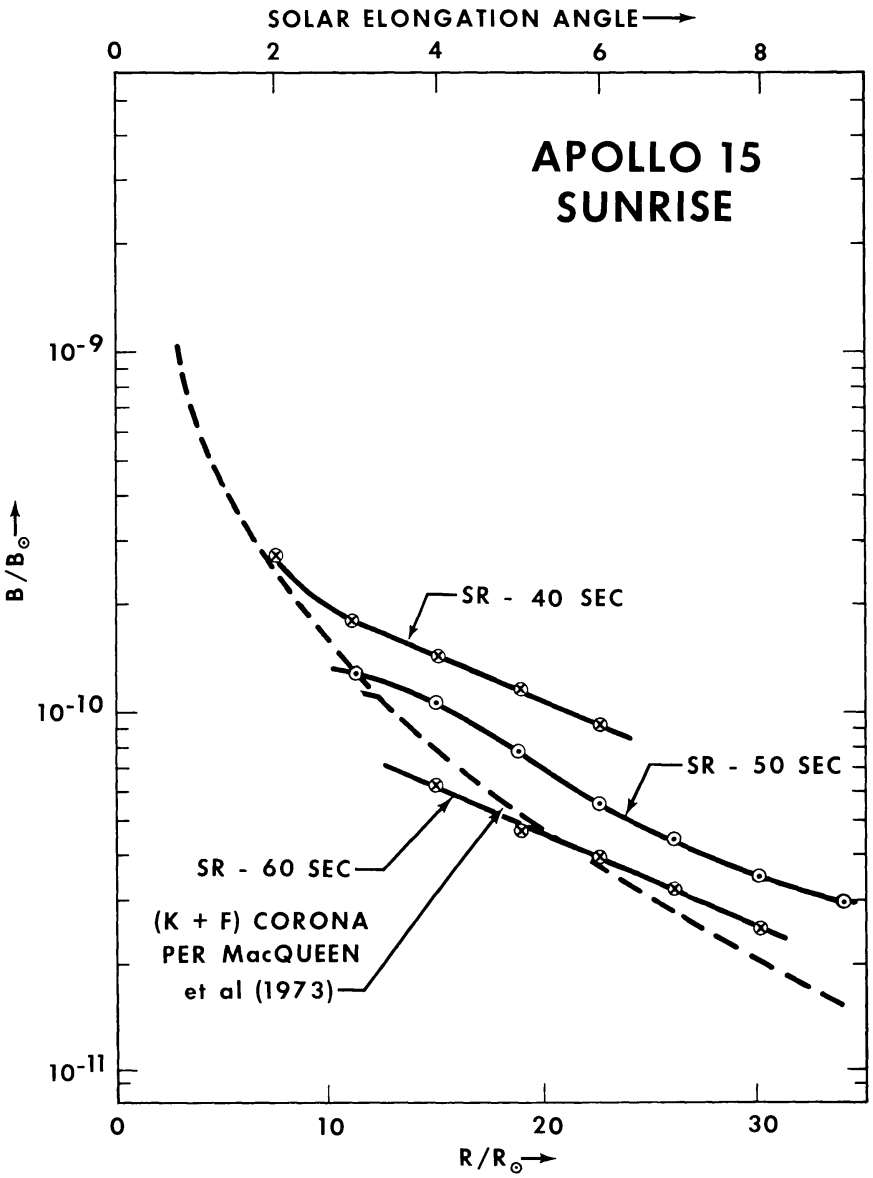

Fig. 2. Observed brightness in "solar corona" images vs. distance from sun center in sequence of 3 photo frames exposed 40, 50, and 60 sec prior to orbital sunrise. Apollo 15 orbit 24; 17:30 GMT, July 31, 1971.

with the Apollo 15 frames where the region of maximum light intensity is entirely offset from the ecliptic. Located above the sub-sun horizon it shows symmetry expected of light scattering from dust particles located above the local lunar terminator, extending to altitudes in excess of 60 km. The inner contours of the Apollo 17 plot (Fig. 4d) should also show this effect, in a manner similar to but less pronounced than the Apollo 15 sunrise profile (Fig. 4b), but it was lost in the artist's redrawing of the profiles. The behavior shows clearly in Fig. 4b, where the true CZL predominates beyond elongations of 10 degrees. The increasing contribution from local scattering inside 10 degrees progressively shifts the center

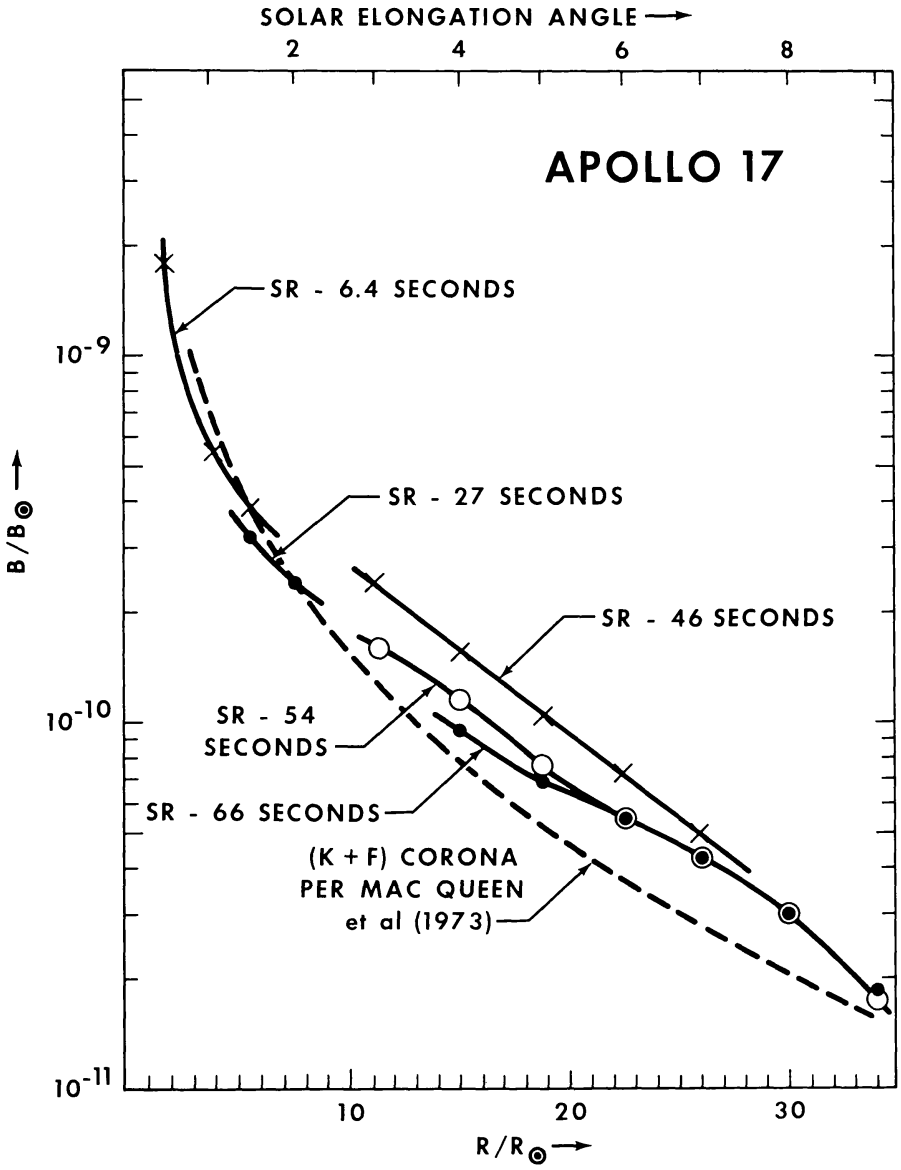

Fig. 3. Observed brightness in "solar corona" images vs. distance from sun center in sequence of 5 photo frames exposed 6-66 sec prior to orbital sunrise. Apollo 17 orbit (26); 20:33 GMT, December 12, 1972.

of intensity off-ecliptic toward the sub-solar symmetry which would prevail with total dominance of the locally scattered light component.

The time development of both spatial symmetry and intensity with elapsed time (distance) from the terminator region can be displayed by a superposition of isointensity contours from successive frames. Figure 5 is a superposition of isointensity profiles from the Apollo 15 sunset frames 318, 320, and 322. The high resolution data set was used, resulting in film graininess showing up as irregularities in (particularly the lower) intensity contours. The positions of the Sun, Venus and the ecliptic plane are constant; with successive positions of the lunar horizon in each frame indicated. Contours from frame 320 (at sunset +33 sec) are

Table 4. Apollo 17—70 mm "solar corona"—sunrise sequence.

Frame No.	AS17-154-23647 (9.9 SEC) SR-66 sec; horiz @ 3.3°				648 (3.9 sec) SR-54 sec; horiz @ 2.7°				649 (1 sec) SR-46 sec; horiz @ 2.3°			
Elongation	*d*	B_0	B_1	*B*	*d*	B_0	B_1	*B*	*d*	B_0	B_1	*B*
3°					1.85	3.5	5.8	15.7	1.52	5.5	9.0	24
4°	1.90	2.1	3.5	9.5	1.70	2.6	4.2	11.4	1.26	3.6	5.7	15.4
5°	1.75	1.6	2.5	6.8	1.50	1.8	2.8	7.6	1.00	2.5	3.8	10.3
6°					1.30	1.3	2.0	5.4	.80	1.8	2.7	7.3
7°	1.42	1.0	1.5	4.1	1.12	1.0	1.5	4.1	.62	1.2	1.8	4.9
8°					.96	.77	1.1	3.0				
9°	1.10	.6	.86	2.3	.80	.6	.8	2.2				
10°	0.95	.5	.7	1.9	.70	.5	.7	1.9				

Frame No.	650 ($\frac{1}{2}$ sec) SR-36 sec; horiz @ 1.8°				651 ($\frac{1}{8}$ sec) SR-27 sec; horiz @ 1.3°				653 ($\frac{1}{60}$ sec) SR-6.4 sec; horiz @ 0.3°			
Elongation	*d*	B_0	B_1	*B*	*d*	B_0	B_1	*B*	*d*	B_0	B_1	*B*
$\frac{1}{2}$°									.80	40	67	180
1°									.47	13	20	54
$1\frac{1}{2}$°					.75	7.0	11.7	32	.43	9	14	38
2°	1.46	7.5	12.5	34	.60	5.4	8.9	24				
3°	1.10	4.6	7.4	20								
4°	.74	2.5	3.9	10.5								
5°	.68	2.2	3.3	8.9								

labeled with their brightness shown in boxes to distinguish them from the other frame contours. Note the overlap of the 8×10^{-10} $B_\odot$ contour at SS + 17 sec (frame 318) with the 3.3 and 5.7×10^{-10} $B_\odot$ contours found later at SS + 33 sec on frame 320. Note particularly the 15–20 degree offset from the ecliptic plane of the direction of symmetry with respect to maximum brightness vs. distance from the sun. This is particularly true of frame 318, which shows the greatest excess brightness. As the excess brightness fades with time, this symmetry is seen to shift slightly toward the solar ecliptic symmetry expected of the background CZL. Although this, or any, symmetry could be displayed at any given time by the K-corona, the K-corona could not display the observed time variation in shape and intensity.

Discussion

Evidence of lunar dust "atmosphere"

The absolute brightness level observed in the Apollo 15 sunset sequence of photos exceeds that of any reported values for the K + F corona by an amount greatly in excess of what could be accounted for by errors in the existing calibration. Even if the observed brightness values could be accounted for by some combination of solar coronal enhancement, calibration errors and possible astronaut errors in setting exposure values, the observed tendency toward lunar

oriented symmetry about the sunset (or sunrise) point, together with the distinct time (i.e., orbital position) dependence of both brightness and symmetry, argues very strongly for a local source of the excess brightness extending several kilometers or more above the lunar terminator regions. Following the same arguments made by McCoy and Criswell (1974) in the case of the Apollo 17 crew observations of "streamers," the most probable source of this excess brightness is the scattering of sunlight by a distribution of very small (probably sub-micron) particles of lunar dust frequently, but not always, present above both dawn and dusk terminators.

"Streamers"—solar coronal or lunar

The time and spatial behavior of the excess brightness observed in the present photographic analysis is similar to that previously inferred from the Apollo 17 crew visual observations of "CZL streamers" which became very prominent within a few seconds of sunrise (or sunset). It was shown (McCoy and Criswell, 1974) that such "streamers" could not be a feature of the solar corona, but must instead be of some origin in the near-lunar vicinity. This raises an important question concerning distinction between true solar coronal features and such features of local origin in any studies made from lunar orbit or the lunar surface.

Although reported to be present during Apollo 15 (D. Scott, pers. comm. and post-flight sketch), no prominent "CZL streamers" of the sort reported by the Apollo 17 crew are evident in the Apollo photos, nor would they be expected as the earliest frames were taken too long after sunset to record their reported maximum intensity. There is a short streamer present in frame 318 which is indicated at about the one o'clock position in Fig. 5. This is one of several in the Apollo 15 photos which have been interpreted as extensions of the well-known inner K-corona structure (Wilson and MacQueen, 1974), due to increases in the solar coronal electron densities. Such features undoubtedly exist, and until now most researchers have assumed that any structure observed in the solar corona/zodiacal light must be due to such K-coronal electron enhancement. Therefore, in any studies made from the lunar surface or lunar orbit, it is important to provide careful distinction between true solar coronal features and features existing in any superimposed light scattered from local sources. The best basis for such distinction, other than simultaneous observation from a non-lunar location, would seem to be the time scale involved in any changes in brightness or form of the feature. Anything that undergoes noticeable change beyond a 1–2 degree elongation angle in a time period of seconds to minutes (and probably hours) is certainly of local origin, as even the fastest evolving features of the solar corona viewed by experiments on Skylab or OSO (MacQueen *et al.*, 1974) required hours to propagate beyond the 6–10 $R_\odot$ fields of view of these instruments. Features that persist for 1–5 days (13–70 degrees of solar rotation) are probably true solar coronal features. Any feature persisting for more than an hour or two, but less than a day, would require additional consideration.

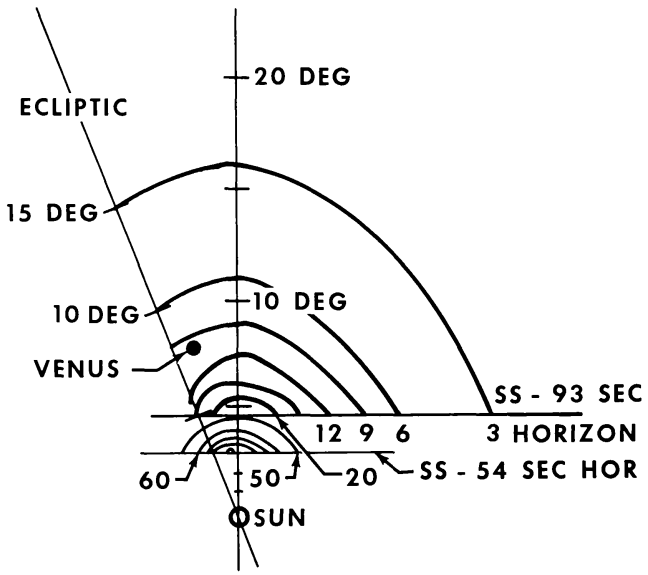

(a)

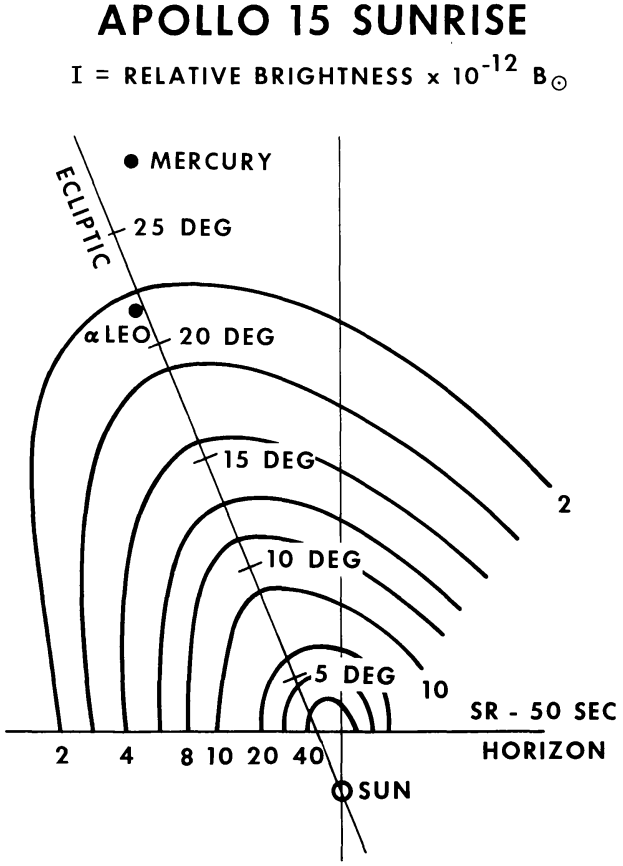

(b)

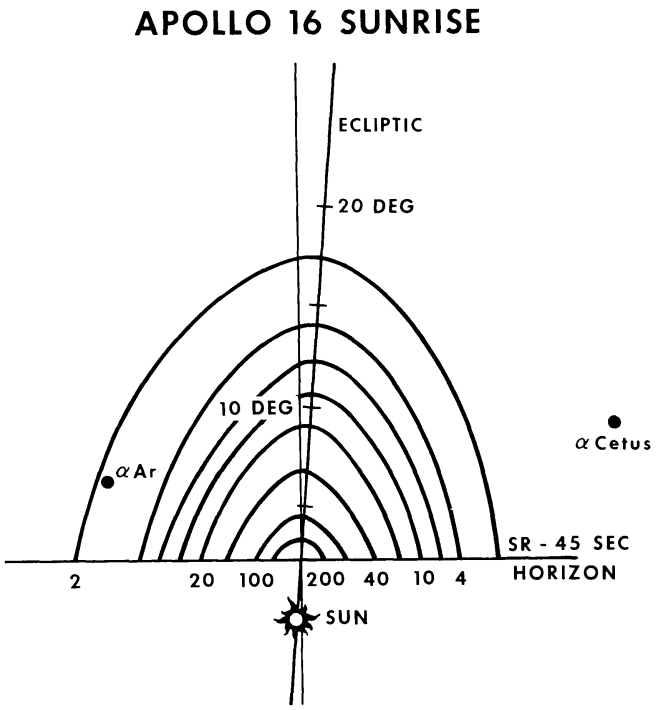

(c)

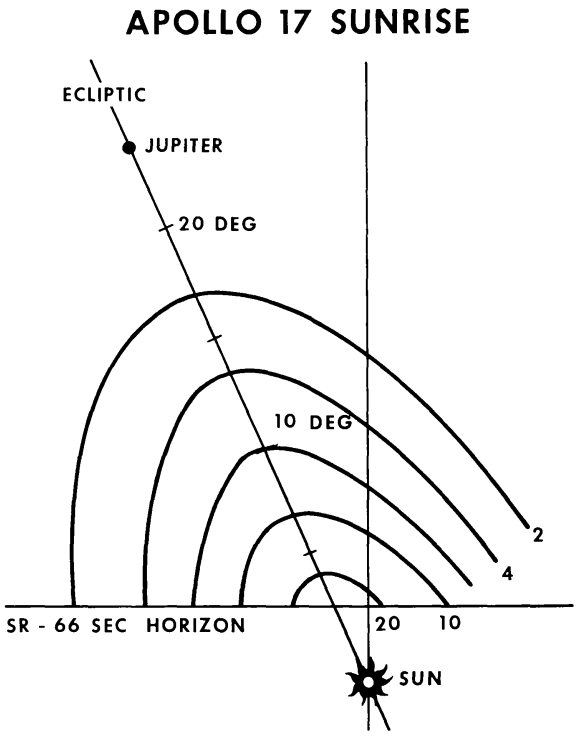

(d)

Fig. 4 (a) AS15-98-13325 isointensity contours; Apollo 15 orbit 24, 93 sec after orbital sunset. Also shows isointensity contours from frame 133222, 54 sec after sunset. (b) AS15-98-13311 isointensity contours; Apollo 15 orbit 24, 50 sec before orbital sunrise. (c) AS16-124-19888 isointensity contours; Apollo 16, orbit 38, 45 sec before sunrise, 22:52 GMT, April 22, 1972. (d) AS17-154-23647 isointensity contours; Apollo 17 orbit 24, 66 sec before sunrise, 17:30 GMT, July 31, 1971.

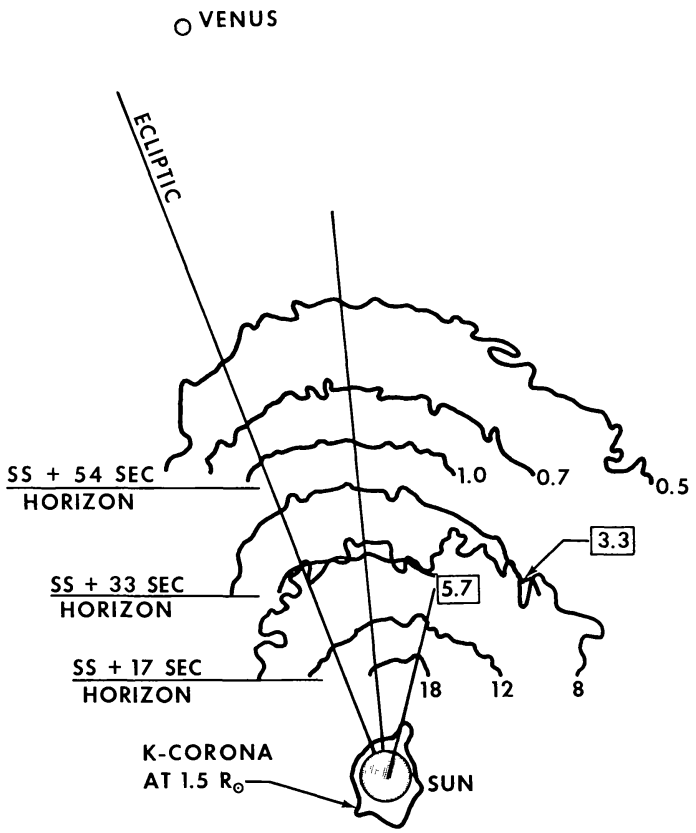

Fig. 5. Superimposed isointensity profiles from time sequence of Apollo 15 "solar corona" images. Inner K-corona brightness profile on the same day (from Wilson and MacQueen, 1974) is also shown for comparison.

Correlation with other observations

The scattered light intensities observed in the Apollo solar corona photographs can be explained on the basis of a distribution of dust particles (Fig. 6) along the line of sight passing above the lunar terminator and/or along the boundary of the lunar shadow. Careful analysis of how this line of sight changes vs. position along the orbit from which each photo was taken may yield a picture of just what size dust is involved and how it is distributed throughout this region. Preliminary models seem to work better if a significant fraction is located immediately along the shadow boundary from the terminator to the intersection with the Apollo orbit suggesting that the particles involved are somehow blown back along this boundary from above (or in front of) the lunar terminator.

Concentrations of lunar atmospheric gases observed by both lunar surface and orbital experiments are entirely too small (Johnson *et al.*, 1972; Hoffman *et al.*, 1973) to give visible scattering of light. Dust present in a lunar "atmosphere" at number densities many times the interplanetary density responsible for the F-corona/zodiacal light can explain the observed scattering of the sun's rays from this region. The possibility of optically significant concentrations of dust at tens to hundreds of kilometers altitude may be correlated with reported observations of

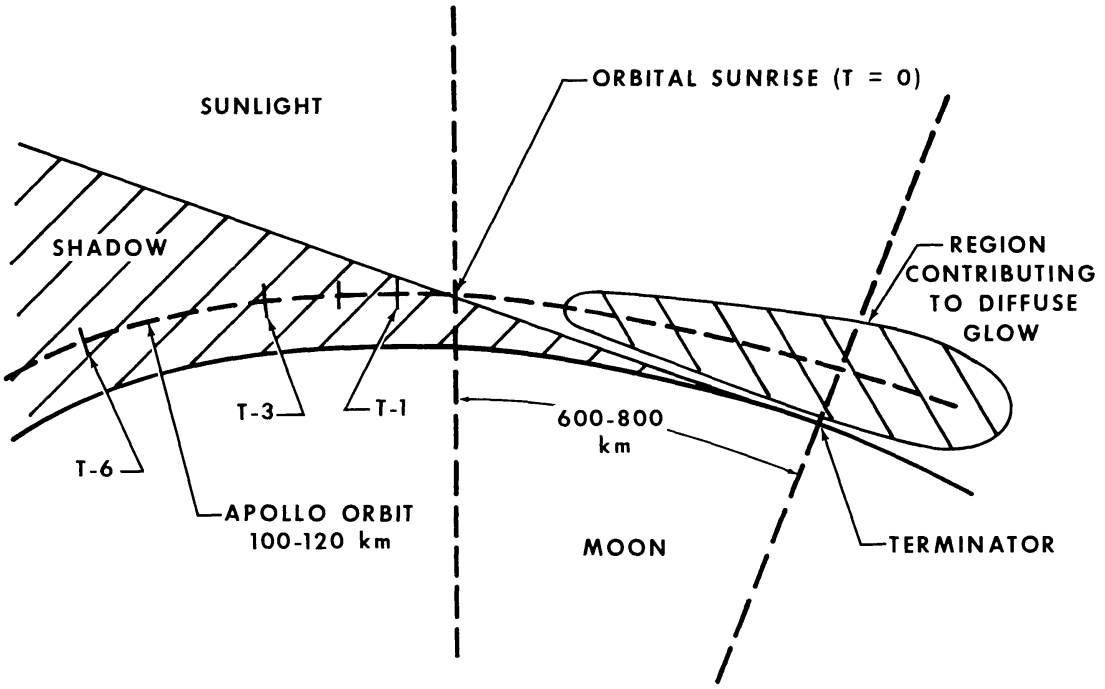

Fig. 6. Schematic cross-section of the moon in the plane of the spacecraft orbit (dashed line). Shows geometry of a physical situation consistent with reported light excess superimposed on view of solar corona from Apollo orbit positions 1–6 min from sunrise/sunset.

dust at lower altitudes. Surveyor observations of a sunset horizon glow have been interpreted in terms of light scattering by very low altitude (10–30 cm above the surface) clouds of dust which are generated by the momentary ejection of lunar fines at flux levels approximately 10^7 times more than estimated for meteoritic secondary ejecta (Criswell, 1972; Rennilson and Criswell, 1974; and references there-in). The analysis of Surveyor attempts to record solar CZL by Bohlin (1971) would seem equally consistent with the present interpretation in terms of local dust scattering rather than his assumption of very broad solar "streamer" structure beyond 20 $R_\odot$. Photometers onboard Lunokhod II (Severny *et al.*, 1973) have observed a strong lunar "twilight" due to ultraviolet and visible light scattering by particles present $\frac{1}{2}$ km or more above the lunar surface (Fig. 7). The LEAM experiment left on the lunar surface to measure size and velocities of cosmic dust, meteoroids, and meteoritic secondaries sees a large number of low velocity particles moving mostly away from the sun for an extended period around every lunar dawn or dusk (Berg *et al.*, 1975). It is not entirely unreasonable or unexpected to interpret the Apollo 15 and 17 observations as light scattering by an even higher altitude distribution of dust.

Electrostatic transport of lunar surface fines (dust) has long been postulated as a major transport mechanism for lunar surface materials (Gold, 1955). However, most of the literature and discussion which evolved from this idea involves movement at altitudes of centimeters above the surface, within the photoelectron layer, and is not particularly relevant to the present observations. Any observa-

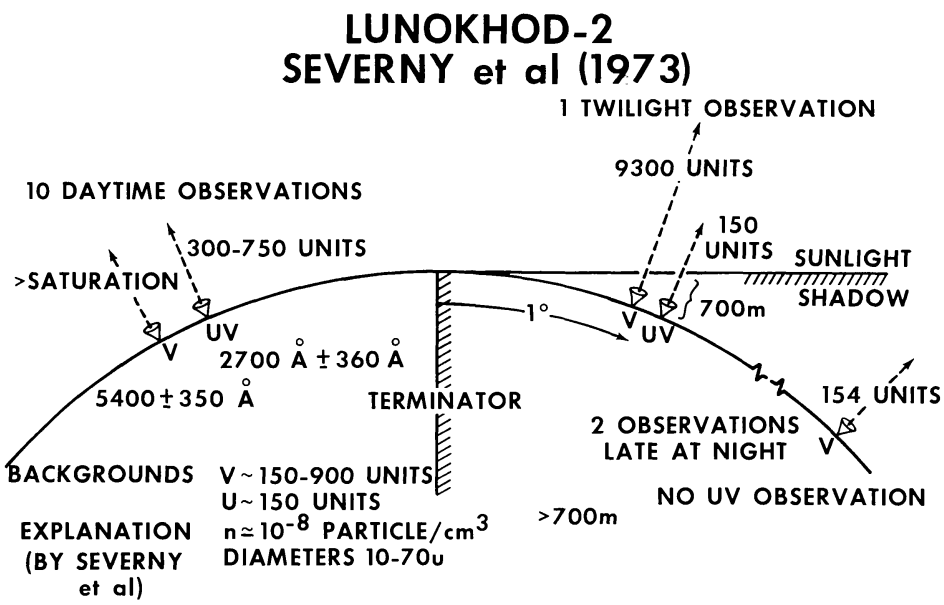

Fig. 7. Illustration of Soviet astrophotometer observations of zenith sky brightness relative to lunar terminator and sunlight/shadow boundary. The unit of brightness is equal to 1 star of mag. 10 per degree^2.

tions of dust at higher altitudes (meters to kilometers) must involve a qualitatively quite different mechanism. The resulting mass transport, erosion, churning and deposition characteristics would presumably be quite different.

Particle number densities

Light scattering by small particles is particularly sensitive to optical properties, particle shape, and orientation. Exact solutions require elaborate calculations using exact values for particle optical properties, size, and shape. Lacking such detailed knowledge and wishing to avoid the theoretical arguments certain to follow any predictions of their properties, the formulas we will use to convert brightness to particle number densities are commonly made (simple) approximations most applicable to nonconducting spherical grains. They give a reasonably good estimate of the angular behavior and number densities to be expected of very simple distributions of the idealized type of particles normally assumed for such calculations. If the actual particles are conducting, have strong optical resonances, or unusual shapes (such as needles or snowflakes), their scattering properties may be very different.

For simplicity, we assume that all the particles are of radius a, scattering incident light of wavelength $\lambda \approx 5{,}000$ Å. Following the methods of van de Hulst (1957), we have for integrated column density of scattering particles along a line of sight

$$N_c = \langle Nd \rangle = \frac{B(\theta)}{F(a, \theta)\pi a^2 E} \tag{1}$$

where E = solar illumination (13.7 lm/cm^2), $F(a, \theta)$ is the scattering efficiency of an individual particle, θ is the solar elongation angle to line of sight, and d is the distance along the line of sight with density N particles/cm^3.

For particles with a $\gtrsim 0.5\ \mu$, we assume nonconducting spheres and use the formula for Fraunhofer diffraction:

$$F(a, \theta) = \frac{X^2}{\pi}\left|\frac{J_1(X \sin\theta)}{X \sin\theta}\right|^2 \qquad \text{where } X = \frac{2\pi a}{\lambda} \tag{2}$$

For particles with a $<0.5\ \mu$, we assume Rayleigh–Gans scattering:

$$F(a, \theta) = 0.006X^4(1 + \cos^2\theta)|G(u)|^2 \tag{3}$$

where $G(u)$ is a function ($u = 2X \sin\theta/2$) qualitatively similar to $J_1(u)/u$. Tabulated values may be found in van de Hulst (1957).

Calculated values of $\langle Nd\rangle$ are shown in Table 5 for particle sizes of 0.1 and

Table 5. $\langle Nd\rangle$ along line of sight over lunar terminator, from Apollo 15 excess brightness in solar corona images.

θ	$\Delta B(\theta)$ cd/cm^2	$\langle Nd\rangle = B(\theta)/E\pi a^2 F(a, \theta)$particles/cm^2	
		$a = 0.1\ \mu$	$a = 1.0\ \mu$
1°	7×10^{-4}	4×10^6	100
3°	8×10^{-5}	5×10^5	20
5°	3×10^{-5}	2×10^5	8
10°	2×10^{-6}	2×10^4	1
20°	2×10^{-7}	2×10^3	2.5

1.0 μ using brightness values taken from the Apollo 15 sunset. We doubt that particles larger than a few microns could be responsible for much of the observed brightness, as the number densities required would be above the upper limit obtained by the Apollo window micrometeoroid results (Cour-Palais, 1974). The column mass required to account for any given brightness is a minimum for $0.1 - 1.0\ \mu$ particles. For larger particles, the Fraunhofer scattering function falls off sharply at angles greater than a few degrees to a ($\lambda/a \sin^3\theta$) dependence, giving a net column mass required to account for the larger elongation angle brightness that increases as a^2. For particles smaller than 0.1 μ, angular dependence becomes small ($G(u) \approx$ constant), scattering efficiency falls off as the sixth power of a, and total mass of scatters required in any column increases as a^{-3}. This effect would seem to rule out any significant contribution by particles much smaller than 0.1 μ.

Figure 8 shows a hypothetical model for a lunar dust "atmosphere", based on the concept shown in Fig. 6, which is capable of providing a zeroth order fit to the Apollo data. This model interprets the observed brightness in terms of a distribution of submicron dust particles above the lunar terminator (and perhaps extending around the sunlit face of the moon); decreasing with altitude to a few

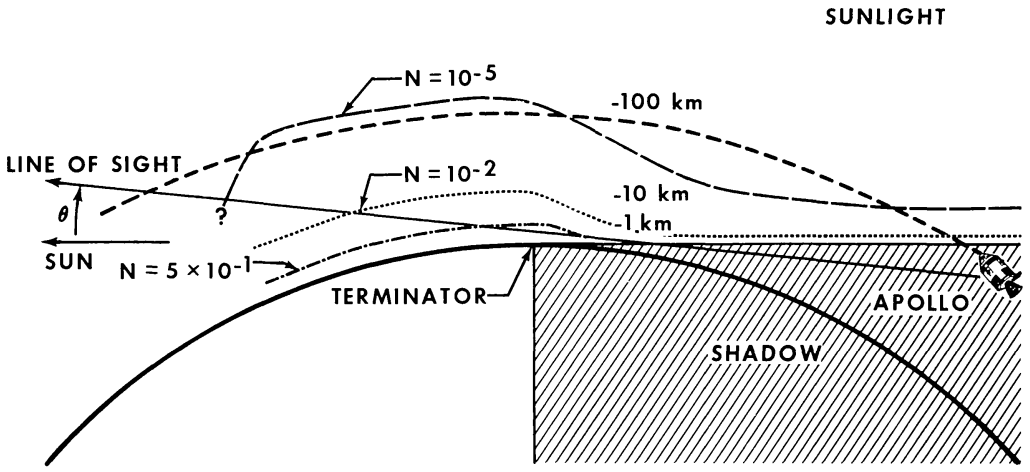

Fig. 8. Model "0"—Shows 2 lines of sight to solar corona through hypothetical distribution of dust above lunar terminator, including layer along sunlight/shadow boundary. Altitude scale above terminator expanded for clarity. Dotted lines are space density contours of 0.1 μ dust (grains/cm^3).

times 10^{-1}/cm^3 at 1 km, 10^{-2}/cm^3 at 10 km, and perhaps 10^{-5}/cm^3 at 100 km. This model also has a layer of particles (5–10%) blown back from over the terminator along the sunlight/shadow interface (by solar wind or radiation pressure?). These number densities are greatly in excess of the concentrations predicted by available analyses for meteoritic secondaries above the lunar surface (Gault *et al.*, 1963), particularly in view of subsequent downward revisions of the estimated micrometeorite flux (Hartung *et al.*, 1972).

The model shown in Fig. 8 will be used in the remainder of this discussion to provide a basis to calculate the implications of our brightness (and the resulting scattering particle density) results in the area of regolith transport processes. All further discussion must, therefore, be qualified by the statement that this model is offered as the best explanation we have found to date for the observed light scattering. It has many difficulties of its own, but fewer than any of the alternatives we have considered. The obvious difficulty of generating so much dust far above the lunar surface is not resolved, but several interesting implications are outlined.

Mass transport and erosion

The model results do not depend on whether the particles are assumed to be on (suborbital) ballistic trajectories, on escape trajectories, or in closed lunar orbits (or otherwise suspended indefinitely above the lunar surface); or for that matter on whether or not they are actually of lunar origin, although the altitude dependence of the model used in Fig. 8 implicitly assumes this. However, if the particles are of lunar origin, the resulting mass transport and lunar removal rates do depend on the type of trajectory the particles follow.

Using an estimated vertical column mass over the terminator of 10^{-9} g/cm^2, we

first estimate the rate of mass churning if this is all in free fall (ballistic trajectory) after ejection from the lunar surface by some process such as meteorite impact. Most of the particles observed at any altitude will be those moving slowly at the top of their trajectories. Therefore, essentially all of the mass/cm^3 at altitude h consists of particles whose total time of flight (surface ejection to secondary impact) is

$$t = \sqrt{\frac{2h}{a}}_{\text{lunar gravity}} \approx 1.2\sqrt{h}$$

where h is in meters. Integrating this over our model column of 10^{-9} g/cm^2 extending to altitudes of greater than 100 km, we get total mass churning rates in excess of 2×10^{-11} g/cm^2 sec. Mass churning to peak altitudes of 10 km would be in excess of 4×10^{-12} g/cm^2 sec, implying mass transport at this rate over distances of 10 km per cycle assuming ejection at random angles and locations as by meteorite impact. Even assuming that this rate applies for only one day/month at the dawn and dusk terminators, this is a rate of greater than 4×10^{-5} g/cm^2 yr. It seems unlikely that we could find a source (or sink) for that much mass moving in ballistic trajectories from either meteoritic secondaries or even Criswell's (1974) terminator dust churning (horizon glow).

High altitude electric fields

Unless most of the observed particles are in closed orbits, which seems highly improbable for any distribution at all like the present model, this almost forces the assumption of some sort of electrostatic suspension of the particles at high altitudes. This assumption increases the individual particles dwell time at altitude, reducing the rate at which particles must enter and leave to sustain the observed population levels. To the extent that the particles are suspended, the mass churning rate would be reduced. Therefore, under the assumption of electrostatic suspension at high altitude, the mass transport rate resulting from the observed particle population could be anything from the maximum calculated above down to zero, depending on the efficiency of suspension over a given region. Even a low rate source such as meteoritic secondary ejection (or a single horizon glow active region) would then be sufficient to sustain a wide range of particle densities at altitude.

The electric fields required to provide some significant degree of suspension are not as wild an idea as they might at first seem. Figure 9 is a plot of field strength required to provide a given ratio of electrostatic force to gravity force on a dust grain of given size and density, under the assumption of photo-electron charging to an equilibrium surface potential of 5 V. The $V \times B$ flow field of the solar wind is too small to have significant effect as are dayside lunar surface fields due to the surface photo-electron layer. However, these fields extend only a few meters above the surface. Above this photo-electron layer both observational (Neugebauer *et al.*, 1972) and theoretical (Siscoe and Goldstein, 1973) evidence

now indicates the existence of potentials exceeding 200 V due to the deflection of solar wind plasma flow in the lunar remnant magnetic fields recently discovered (Coleman *et al.*, 1972; Russel *et al.*, 1975; McCoy *et al.*, 1975a; Anderson *et al.*, 1976) to extend over distances of 1–100 km from the lunar surface. Observed fields at the Apollo 12 site (magnetic field 38 γ reversing in less than 10 km) are in excess of 200 V/10 km = .02 V/m (Clay *et al.*, 1975).

With the (solar wind) plasma flow energy available to drive any other space charge separation effects which might occur, to the extent they are not shorted out by the ambient plasma, it would appear likely to find quite a variety of electric field configurations entangled within the ambient lunar magnetic fields above the lunar daytime surface, and perhaps along the lunar shadow and solar wind plasma void boundary. To my knowledge, no definitive theoretical treatment exists to calculate the potentials necessary to match current flows across this boundary. Formation of significant potential drops across such an interface seems probable. Net potential drops of the order of − 100 V (over 1 km) are observed at the lunar terminator by the SIDE experiment (Benson *et al.*, 1975). Potentials of a few hundred volts (with the opposite polarity) may be responsible for edge effects in the energetic electron flux decreases inside the plasma void observed by the PFS lunar satellites (Anderson *et al.*, 1972).

The preceding discussion of high altitude electric field generation above the lunar surface is intended to be neither definitive nor complete, but rather to illustrate that the existence of such fields would not be unreasonable. The theory involved becomes quite complex. Their existence would provide a good physical mechanism to explain the observed light scattering. If they, in fact, do not exist; then some other means must be found to spread more than 10^{-9} g/cm^2 of dust to altitudes exceeding 100 km in order to account for the light scattering observed in

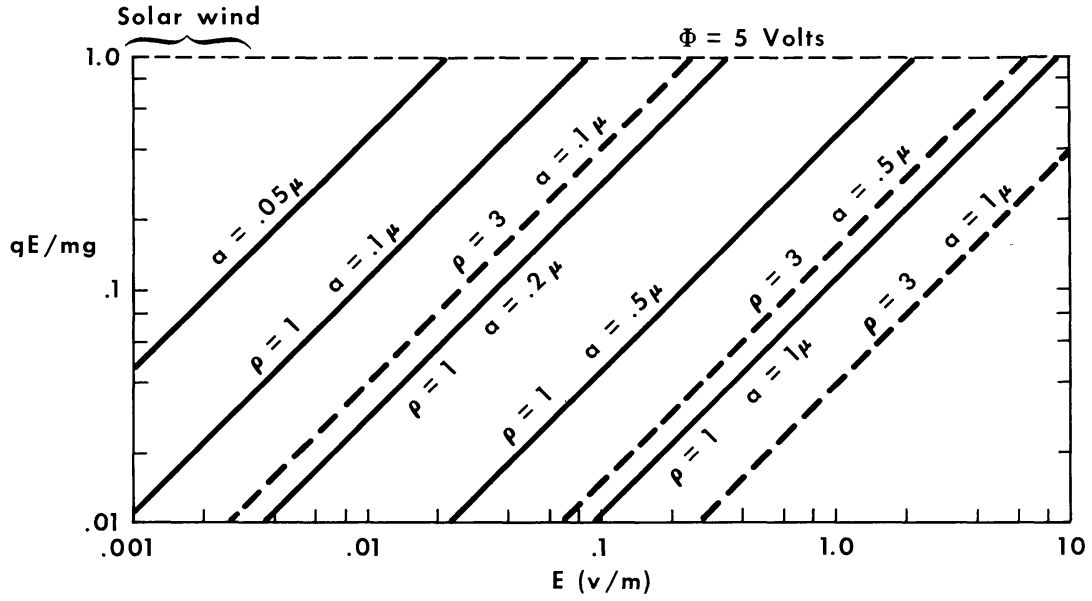

Fig. 9. Ratio of electrostatic to gravitational force on particles charged to +5 V potential vs. ambient electric field.

the Apollo photography. If they do exist, and presumably would have some sort of coherent pattern, this would result in transport of particles along preferred paths; leading to preferential erosion or deposition of the lunar fines involved at particular points on the lunar surface, rather than random redistribution as in the case with meteor impact or other purely ballistic processes.

Spacecraft contamination—Are the particles "yellow snow"?

A co-orbiting cloud of contaminants from the Apollo vehicle itself might provide the particle densities needed to scatter quite a bit of light, especially just prior to orbital sunrise or after orbital sunset, without requiring a major revision of our ideas of small particle population densities and behavior many kilometers above the lunar surface. The Apollo vehicle provides several sources for such contaminants; snowflakes formed from waste water or urine dumps and exhaust products from engine or thruster firings, just to name a few known to dump many pounds of contaminants into space from Apollo. As may be seen from Table 5, a few grams of material would be sufficient to give the observed scattering if it were concentrated near the Apollo vehicle.

However, light scattering from this cloud of contaminants would not account for the observations. Although such a cloud would indeed brighten suddenly as it entered the lighted region just ahead of the Apollo, it would first catch the sunlight at a point above rather than in front of the spacecraft. This can be easily visualized by referring to the T-1 minute position in Fig. 6 and imaging a small spherical contamination cloud about that point. Even with the strong angular dependence of forward diffraction shown by Eqs. 2 and 3, the observed brightening would be originally overhead (above the 20° point where orbit intercepts sunlight), progressing toward the horizon rather than vice versa as observed. Scattering from such a cloud, therefore, might contribute to but not dominate the observed scattering. Duplication of the observed brightness profiles would require a particle cloud becoming denser below the Apollo orbit, thinner above. This does not seem dynamically reasonable.

Hoffman *et al.* (1972) give observational evidence of the existence of a co-orbiting cloud of contaminants detectable by the onboard mass spectrometer, however it would not seem to provide either sufficient gas or particles to scatter much light. Nauman (1972) reports that high sensitivity photography during and following a waste water dump showed a total brightness during the actual dump in full solar illumination, which never exceeded $6 \times 10^{-10}\ B_\odot$. He also puts an upper limit on light contamination plus any residual contamination cloud one hour after the dump of $5 \times 10^{-13}\ B_\odot$ at $\epsilon = 90°$. The cloud of contaminants would appear to disperse too quickly to co-orbit in the vicinity of Apollo. Therefore, direct observational evidence also argues against any co-orbiting cloud as the major source of the observed brightness.

A more thoroughly dispersed contamination of the entire orbital region would be impossible to distinguish from particles arriving in the area via natural means. Integrated vertical column densities of 10^{-9} g/cm^2 would require 10 g/km^2 along

the orbit. Therefore, to so populate a swath 50 km (5° at 600 km range) to either side of the orbit would require a total of 10^4 kg. This does not seem reasonable, unless the number could be reduced by assuming the particles form in a snowflake configuration requiring much less mass to provide the same scattering efficiency. However, even if it were all in "snowflakes" it is hard to understand why it would stay in the very low and circular orbits which seem required to provide the observed angular dependence of brightness. If it stayed in the original Apollo orbit, or a simple perturbation thereof, it would not provide the apparent altitude dependence observed. This concept would also have difficulty explaining the difference in scattered light intensities between the Apollo 15 sunset sequence and the sunrise sequence taken 1 hr earlier on the other side of the moon (without invoking high altitude electric fields or some other mechanism to preferentially provide greater densities over one region than another). There were no urine dumps or major engine firings for several hours prior.

Similar vertical column densities were calculated by McCoy and Criswell (1974) from the Soviet Lunokhod II data (Severny *et al.*, 1973) for zenith sky brightness 2 hr after sunset. It has been pointed out by one of the referees that contamination from Apollo could probably be ruled out for this observation.

Implications of variability

The fact that different scattered intensities were observed during Apollo 17 than were observed on Apollo 16 or 15 is significant in that it requires the population of these particles, whatever their source, to be variable in nature. Though apparently a common occurrence, there are times when the scattering as seen by Apollo 15 and 17 is either not present or reduced by more than a factor of ten. In fact, the difference between the Apollo 15 sunset and sunrise observations requires change by a factor of two or more in either 1 hr or from one terminator to the other.

Either possibility, change in less than an hour or from place to place above the lunar surface, not only argues against moon-wide contamination by the Apollo vehicle itself as a source, but probably precludes meteoritic secondaries in ballistic free-fall as an explanation of the observed light scattering. Unless the input term (meteoroid flux) can be shown to change that much, or the micron size secondary population dominated frequently by a momentarily present cloud of secondaries from a single large primary, then the only way to match either source to variable observations is by assuming a storage (electrostatic suspension?) function that can modulate the constant input term to provide the observed variable particle density.

Removal of mass from the moon

To the extent that particles are suspended for longer dwell times above the lunar limb, the time available for solar wind or radiation pressure to sweep them downstream away from the region is increased. That this actually occurs is

suggested by both the tendency of the zero order particle distribution model to match the observed scattering behavior better if it includes a population of dust grains downstream from the terminator along the lunar shadow boundary and by the LEAM results (Berg *et al.*, 1975) which record velocities predominantly away from the sun for the particles it observes during both lunar surface sunrise and sunset. As an example, if the smaller or lighter particles in the 10^{-9} g/cm^2 vertical column are removed with 1% efficiency by some mechanism (such as photoelectric supercharging and resulting acceleration by the solar wind field) operating to produce a mean dwell time of 1000 sec for the particles removed, the result would be the net removal from the moon of 10^{-14} g/cm^2 sec of lunar surface fines. Depending upon the actual percent efficiency and time scale for removal, the actual rates could be anything from zero up to perhaps 10^{-13} g/cm^2 sec (it seems unlikely that removal efficiency would much exceed 10%, nor the process require less than 1000 sec).

Using the 10^{-13} g/cm^2 sec as a probable upper limit estimate, and assuming the escape would only come from the region within 10 degrees of each terminator, this would predict a net removal of as much as 10^{-8} g/cm^2/month averaged over the entire lunar surface. This translates to 4×10^7 kg/yr lost from the entire moon, or an average of 0.5 mm of density 2 g/cm^3 surface fines per million years. This might be removed uniformly over the lunar surface, but more likely would come preferentially from certain regions with particularly favorable field configurations to feed the process. Other regions of the lunar surface could at the same time experience a large net deposition of fines falling back to the surface.

The preceding calculations are not intended to be definitive. They are very rough order of magnitude estimates, intended only to demonstrate the *possible* importance of this phenomena to the geochemistry and geophysics of the lunar regolith fines if it in fact operates with anything near to its potential efficiency. The rates of removal calculated above, or the rates of transport calculated earlier, would be capable of significantly altering soil maturation processes by removing (or adding to) certain regolith fines at rates capable of exceeding their total rate of generation.

Conclusions

The Apollo 15 and 17 seventy mm solar corona photo sequences show evidence of the presence of an anomalous component of brightness in each image, superimposed on the light from the true solar corona. The source of this additional light would appear to be scattering of sunlight by small particles along the line of sight toward the sun, passing at altitudes of 1–100 km above the terminator. The key observations supporting this anomalous scattering of sunlight near the lunar surface are: (1) The apparent brightness of the "corona" at a *given elongation* is a function of (time or) the position of the observer relative to the terminator. (2) The isophotes of the "corona" above the lunar horizon drift away from ecliptic plane symmetry toward symmetry with respect to a line perpendicular to the lunar horizon as the line-of-sight approaches the horizon. (3) Matching the observed

variation in brightness with solar elongation angle and observer position requires an increase in density of scatterers with altitude below the spacecraft orbit for any of the simple models calculated.

Careful cross-checking of the film calibrations indicate that the relative image brightness values are reliable to ±10%. Cumulative uncertainties in window/lens transmission values, film spectral response, and effect of radiation fog pre-exposure sensitization of the film result in about 60% uncertainty in absolute calibration. This would not significantly modify the present results, as it would be a constant shift in log brightness of all points, leaving the characteristic relative behavior unchanged. The possibility that the astronauts somehow mis-set the exposure on some of the frames cannot be ruled out absolutely; however, there is no way to make the apparent brightness at constant elongation match in all frames by assuming a series of simple mistakes (like using $\frac{1}{8}$ sec instead of $\frac{1}{4}$ sec, etc.). The present assumption of an additional (steadily increasing) component of locally scattered light does fit the data well and would appear to be correct.

Assuming the estimates of lunar sky brightness are correct, the observed excess brightness and symmetry are consistent with diffraction scattering by small particles at altitudes of 1–100 km (or more) above the lunar surface. The particles are presumed to be lunar surface fines (dust) in the size range 0.1–1 μ. Larger or smaller solid particles are less likely, due to both the greater total mass of such sizes needed to give the observed scattering intensity and the observed angular intensity variations.

Snowflakes or CO_2 crystals (which should sublime rapidly) also seem less likely than solid grains (although some do seem to be present) due to the low level of their respective gas molecules observed by the orbital and surface experiments.

A co-orbiting spherical cloud of spacecraft contaminants would not produce the angular brightness behavior observed, nor would it be consistent with reported direct photographic observation of brightness and dispersion rates during an intentional waste water dump from Apollo 15. A more extended distribution of contaminants, in orbits mostly below Apollo, can not be ruled out; but such contaminants would have several difficulties in reproducing all of the observed behavior.

The model presented in Fig. 8 is used to provide working estimates of the implications of the observed excess brightness. Its essential features are a strong gradient in particle density over the lunar terminator, with particles concentrated toward lower (10–1 km) altitudes. A secondary, but inconclusive, feature is a thin layer of particles along the solar shadow boundary. The distribution to be used on the sunward side of the moon from the terminator is indeterminant. The model is used as a basis for discussion because it is the only simple model which roughly reproduces the observed brightnesses (i.e., it comes closer than similar simple models with the particles concentrated in a cloud around the spacecraft or along the orbit.) It has no further merit and should not be taken as more than an order of magnitude starting point.

The immediately obvious difficulty with this hypothesis is the great difficulty in accounting for so much dust far above the lunar surface. Meteoritic secondaries in

ballistic trajectories would imply mass churning (turn-over) rates exceeding 4×10^{-12} g/cm^2 sec (10^{-4} g/cm^2 yr) to altitudes of exceeding 10 km (10^{-3} g/cm^2 yr above 1 km). These are far in excess of current estimates. If the brightness estimates and resulting model are at all correct (the alternatives we have checked have even greater difficulties), then this almost forces the assumption of some sort of suspension of the particles to increase their dwell time at high altitude; thus reducing the turn-over rate associated with a given number density along any line of sight. Electrostatic suspension of charged grains by high altitude electric fields of some unspecified origin would seem to be the least unlikely means of accomplishing this. Recent experimental results do, at least, indicate the presence of some fields approaching the magnitude and altitude extent required. Whether or not these, or fields from some other source yet unnoticed, are actually effective in providing the hypothetical suspension is a question that will require extensive further development of our understanding of such fields before an answer can be given.

If such high altitude suspension of lunar surface fines is, in fact, effective, it would reduce the regolith mass churning rate implied by the number densities at 1–100 km downward from 10^{-3} g/cm^2 yr toward zero. The actual rate would be dependent upon the efficiency of suspension above any given region, probably resulting in selective erosion from some areas and deposition in others of soil fines. The period of suspension would also increase the probability of some of the suspended fines being swept away from the moon entirely. Again, the rate could be anything from zero to more than 10^{-8} g/cm^2 month (0.5 mm of density 2 g/cm^3 surface fines per million years). If present, such effects should show up in their effects on soil maturation processes and small size populations.

Acknowledgments—The author wishes to thank R. M. MacQueen, C. L. Ross, and R. D. Mercer for providing the original 70 mm flight films and HAO calibration data for use in this analysis. I also thank Bob Gooding and the JSC Photographic Sciences Office for performing the microdensitometer scans of the flight film and providing JSC calibration data. I am indebted for many useful discussions with D. Criswell of the Lunar Science Institute and C. Ross of the High Altitude Observatory.

References

Anderson K. A., Chase L. M., Lin R. P., McCoy J. E., and MacGuire R. E. (1972) Solar wind and interplanetary electron measurements on the Apollo 15 subsatellite. *J. Geophys. Res.* **72**, 4611–4626.

Anderson K. A., Lin R. P., McCoy J. E., McGuire R. E., Russell C. T., and Coleman P. J. (1976) The large magnetized region associated with Rima Susalis (abstract). In *Lunar Science VII*, p. 16–18. The Lunar Science Institute, Houston.

Benson J., Freeman J. W., and Hills H. K. (1975) The lunar terminator ionosphere. *Proc. Lunar Sci. Conf. 6th*, p. 3013–3021.

Berg O. E., Wolf H., and Rhee J. (1975) Lunar soil movement registered by the Apollo 17 cosmic dust experiment, IAU Colloqium #31. Heidelberg, Germany, June 13. Preprint.

Bohlin J. D. (1971) Photometry of the outer solar corona from lunar-based observations. *Solar Physics* **18**, 450–457.

Clay D. R., Goldstein B. E., Neugerbauer M., and Snyder C. W. (1975) Lunar surface solar wind observations at the Apollo 12 and 15 sites. *J. Geophys. Res.* **80**, 1751–1760.

Coleman P. J., Jr., Lichtenstein B. R., Russell C. T., Sharp L. R., and Schubert G. (1972) Magnetic fields near the the moon. *Proc. Lunar Sci. Conf. 3rd*, p. 2271–2286.

Cour-Palais B. (1974) The flux of meteoroids at the moon in the mass range 10^{-8} to 10^{-2} G from the Apollo window and Surveyor-III TV camera results (abstract). In *Lunar Science V*, p. 138–140. The Lunar Science Institute, Houston.

Criswell D. R. (1972) Lunar dust motion. *Proc. Lunar Sci. Conf. 3rd*, p. 2671–2680.

Criswell D. R. (1974) Horizon-glow and the motion of lunar dust. In *Photon and Particle Interactions with Surfaces in Space* (R. Giard, ed.), p. 545–556. D. Reidel, Dordrecht, Holland.

Dunkelman R., Mercer R. D., Ross C. L., and Worden A. (1974) Astronomical photography. In *Apollo 15 Prelim. Sci. Rep.*, NASA publication SP-289, p. 25-108 to 25-112.

Gault D. E., Shoemaker E. M., and Moore H. J. (1963) Spray ejected from the lunar surface by meteoroid impact. NASA publication D-1767.

Gold T. (1958) The lunar surface. *Monthly Not. Royal Astron. Soc.* **115**, 585.

Hartung J. G., Horz F., and Gault D. E. (1972) The origin and significance of lunar microcraters. *Proc. Lunar Sci. Conf. 3rd*, p. 2735–2753.

Hodges R. R., Hoffman J. H., and Johnson F. S. (1973) Composition and dynamics of the lunar atmosphere. *Proc. Lunar Sci. Conf. 4th*, p. 2855–2864.

Hoffman J. H., Hodges R. R., Johnson F. S., and Evans D. E. (1973) Lunar atmospheric composition results from Apollo 17. *Proc. Lunar Sci. Conf., 4th*, p. 2865–2875.

Hoffman J. H., Hodges R. R., and Evans D. E. (1972) Lunar orbital mass spectrometer experiment. *Proc. Lunar Sci. Conf. 3rd*, p. 2205–2216.

Johnson F. S., Carroll J. M., and Evans D. E. (1972) Lunar atmosphere measurements. *Proc. Lunar Sci. Conf. 3rd*, p. 2231–2242.

Hundhausen A. J. (1970) Composition and dynamics of the solar wind plasma. *Rev. Geophys. Space Phys.* **8**, 729–811.

MacQueen R. M., Eddy J. A., Gosling J. T., Hildner E., Munro R. H., Newkirk G. A., Poland A. I., and Ross C. L. (1974) The outer solar corona as observed from Skylab: Preliminary results. *Astrophys. J.*, **187**, L85–L88.

MacQueen R. M., Ross C. L., and Evans R. E. (1973) Part B—Solar corona photography. In *Apollo 17 Prelim. Sci. Rep.*, NASA publication SP-330, p. 34-4 to 34-6.

MacQueen R. M., Ross C. L., and Mattingly T. K. (1973a) Observations from space of the solar corona/inner zodiacal light. *Planet. Space Sci.* **21**, 2173–2179.

McCoy J. E. and Criswell D. R. (1974) Evidence for a high-altitude distribution of lunar dust. *Proc. Lunar Sci. Conf. 5th*, p. 2991–3005.

McCoy J. E., Ross C. L., and Criswell D. R. (1975) Photometric evidence of light scattering above the lunar terminator from Apollo orbital corona photography (abstract). In *Lunar Science VI*, p. 537–539. The Lunar Science Institute, Houston.

McCoy J. E., Anderson K. A., Lin R. P., Howe H. C., and McGuire R. E. (1975a) Lunar remnant magnetic field mapping from orbital observations of mirrored electrons. *The Moon* **14**, 35–47.

Naumann R. J. (1972) Contamination photography. NASA publication TMX-64681.

Neugebauer M., Snyder C. W., Clay D. R., and Goldstein B. E. (1972) Solar wind observations on the lunar surface with the Apollo 12 ALSEP. *Planet. Space Sci.* **20**, 1577–1591.

Pizzo V. and Gosling J. T. (1972) A sensitometer box for solar corona photometry. *AAS Photo. Bull.*, **1**, 19–21.

Rennilson J. J. and Criswell D. R. (1974) Surveyor observations of lunar horizon glow. *The Moon* **10**, 121–142.

Russell C. T., Coleman P. J., and Schubert G. (1975) The Lunar magnetic field. In *Space Research XV* In press.

Severny A. B., Terez E. I., and Zvereva A. M. (1973) Preliminary results obtained with astrophotometer installed on Lunokhod-2. In *Space Research XIV*, p. 603–605. Akademie-Verlag, Berlin. In press.

Siscoe G. L. and Goldstein B. E. (1973) Solar wind interaction with lunar magnetic fields. *J. Geophys. Res.* **78**, 6741–6748.

Van de Hulst H. C. (1957) *Light Scattering by Small Particles.* John Wiley, New York. 470 pp.

Wilson D. C. and MacQueen R. M. (1974) Observed streamer curvature in the outer solar corona. *J. Geophys. Res.* **79**, 4575–4580.